Accurate Prediction of Ferrite Core Loss with Nonsinusoidal Waveforms Using Only Steinmetz Parameters

K. Venkatachalam
C. R. Sullivan
T. Abdallah
H. Tacca

Accurate Prediction of Ferrite Core Loss with Nonsinusoidal Waveforms Using Only Steinmetz Parameters

Kapil Venkatachalam, Charles R. Sullivan, Tarek Abdallah, and Hernán Tacca*

kapil.venkatachalam@dartmouth.edu, charles.r.sullivan@dartmouth.edu, Tarek.A.Abdallah.Th02@Alum.Dartmouth.ORG,
htacca@ieee.org, http://engineering.dartmouth.edu/inductor

Thayer School of Engineering, Dartmouth College, Hanover, NH 03755, USA

*Depto. de Electrónica Fac. de Ingeniería, Universidad de Buenos Aires, 1063 Buenos Aires, Argentina

Abstract— **An improved calculation of ferrite core loss for nonsinusoidal waveforms separates a flux trajectory into major and minor loops via a new recursive algorithm. It is highly accurate and outperforms two previous methods for our measured data. The only characteristics of the material required are the standard Steinmetz-equation parameters.**

I. INTRODUCTION

FOR computer-aided design (CAD) of magnetic power devices, including electric machines, transformers, inductors, and other static reactors, an accurate prediction of loss in magnetic materials is essential. A widely used calculation is a power law equation [1], [2]

$$\overline{P_v(t)} = k f^\alpha \hat{B}^\beta \qquad (1)$$

where $\hat{B}$ is the peak flux amplitude, $\overline{P_v(t)}$ is the time-average power loss per unit volume, and f is the frequency of sinusoidal excitation, and k, α, and β are constants found by curve fitting. A similar equation, but without the frequency dependence, was proposed by Steinmetz in 1892 [3], and so (1) is often referred to as the Steinmetz equation. Unfortunately, the Steinmetz equation, as well as the data provided by manufacturers of magnetic materials, is based only on sinusoidal excitation, whereas switching power converters and, increasingly, electric machines, can have very different waveforms. These nonsinusoidal waveforms result in different losses [4], [5], [6]. DC bias can also significantly affect loss [7], [8], [9]. A better method of determining loss, accurate for a wider variety of waveforms, is needed. Our work is motivated primarily by applications to MnZn power ferrite materials. However, the results may be useful for other materials as well.

More detailed models, based on physical phenomena producing loss, have been studied [10], [11], [12], [13], [14], [15], [16], [17], [18], [12], [13]. However, especially for ferrites, there is not yet a clear consensus on a practical physically-based model that properly includes dynamic and nonlinear effects [6]. Furthermore, the physically-based models that appear most promising require additional characterization well beyond what is typically available in manufacturers' data sheets, and it is unlikely that design engineers will typically undertake the necessary measurements and parameter extraction.

Two recent models use the Steinmetz equation parameters, but extend the calculation to address arbitrary waveforms: the "modified Steinmetz equation" (MSE) [4], [5], [19], and the "generalized Steinmetz equation" (GSE) [6]. Another similar model was developed in [20]. In [6] the GSE is introduced to overcome anomalies in the MSE. As is discussed in Section I-A, the model introduced in [20] also exhibits anomalies. In [6], the MSE and GSE are compared with experimental data, and while both provide a vastly better approximation than the basic Steinmetz equation (1), and the GSE avoids some problems exhibited in the MSE, each has significant error in at least one region.

A careful examination of the data in [6] shows that where the GSE model deviates from the measured data is very close to the point at which the flux waveform ceases to be monotonic–that is, where it starts to contain minor hysteresis loops. Thus, in order to improve on those results, we have studied the possibility of separating the flux waveform into major and minor loops, and calculating the loss separately for the major loop and for each minor loop. This loop separation does not directly improve the performance of the GSE, because the GSE is based on a hypothesis about instantaneous power dissipation that is unaffected by whether a section of the waveform is considered as part of a minor loop or not. Thus, in order to make use of separated loops to improve the accuracy of the GSE, the calculation of loss for each separate loop must be something different from the original GSE. We find that an expression similar to the GSE, but based on peak-to-peak amplitude of the major or minor loop under consideration, works well when used with separation of minor loops.

In Section II-A we describe the modification of the GSE to make it depend on peak-to-peak amplitude. In Section II-B, we describe the recursive algorithm we developed that can separate any number of nested or separate minor loops and sub-loops. In Section III, we compare the results of the improved model with experimental data.

A. Criteria for a Self-Consistent Loss Model

Without a strong theoretical basis for a nonlinear, dynamic loss model, a vast number of formulations are possible. Fortunately, many possibilities can be dismissed as implausible even without experimental measurements. To define several

criteria that must be met for a plausible solution we propose two axioms:

Axiom 1: The loss must be a continuous function of parameters describing the waveform.

Axiom 2: If there are two equivalent descriptions of a waveform, calculations of loss based on either must give the same result.

In [6], the MSE [5] is shown to violate these axioms. The period of the waveform is important in the calculation of the MSE. But a slight, unimportant change of parameters of a waveform can result in a jump in the period. For example, the flux waveform $B(t) = B_0(\epsilon \sin(\omega t) + \sin(10\omega t))$ jumps by a factor of ten as ϵ goes from zero to infinitesimally greater than zero. Thus, the loss is a discontinuous function of a continuous change of a parameter of the waveform. The relation between the two axioms can be seen by considering the case in which $\epsilon = 0$. The waveform may be described as periodic with period $T = \frac{2\pi}{\omega}$ or $T = \frac{2\pi}{10\omega}$. This may seem to be a purely academic point, but it leads directly to the discontinuity problem. As shown in [6], it is also related to the mismatch between the MSE and measured data.

The model proposed in [20] calculates loss for a piecewise linear (PWL) flux waveform as

$$\overline{P_v} = k_w \sum_i \left\{ |B_{i+1} - B_i|^m \left[2(t_{i+1} - t_i)\right]^{-n} \frac{t_{i+1} - t_i}{T} \right\} \tag{2}$$

where B_i are the flux values at times t_i, m, n, and k_w are constants that [20] recommends finding from measurements with squarewave excitation, and $\overline{P_v}$ is the time-average power dissipation per unit volume.

This violates Axiom 2 in that if a segment of the PWL waveform is divided into two consecutive segments (with equal slope), (2) gives a different result, as

$$2 \left|\frac{1}{2}\right|^m \left[\frac{1}{2}\right]^{-n} \frac{1}{2} \neq 1 \tag{3}$$

unless $n = m$.

One could stipulate that no single segment be divided, in an attempt to circumvent Axiom 2, but as with the MSE, the violation of Axiom 2 is associated with a violation of Axiom 1 as well. An infinitesimal change in slope at the midpoint of a segment would necessitate separation into two segments, hence causing a jump in the calculated loss.

Although the intent of [20] was only to model PWL waveforms, not more general waveforms, consideration of how it would apply clarifies the difficulties it poses. If one were to calculate loss for a smoothly curving waveform, one would hope to be able to derive better and better results by approximating it with more and more time segments. However, as demonstrated by (3), each time more segments are used, the loss changes. With $m > n$, as is typically the case, the result decreases as a finer approximation is used, with the loss approaching zero in the limit of an infinite number of segments.

The consideration of these Axioms 1 and 2 allows one to see that the MSE [5] and the model in [20] cannot be expected to work well for truly general consideration of many different possible waveforms; the problems with the MSE were confirmed experimentally in [5]. Thus, in developing improved models, it is important to heed the axioms.

II. IMPROVED LOSS MODEL

A. Modifying the GSE

The GSE was developed on the basis of a general hypothesis for instantaneous core loss, [21]

$$P_v(t) = P_d(\frac{dB}{dt}, B) \tag{4}$$

where P_d is an unknown power dissipation function. This formulation is not well justified: Assuming that P_d is a single-valued function of dB/dt and B oversimplifies the actual physical phenomena that, in general, depend on the time-history of the flux waveform as well as on its instantaneous value and derivative [11], [22]. Thus, with such a formulation, it should not be surprising if there are situations in which it is not accurate. Also note that splitting the flux trajectory into major and minor loops should not make any difference for any loss calculation that can be expressed as (4).

In [6], it is shown that (4) is consistent with the Steinmetz equation for sinusoidal waveforms if the particular loss function used is

$$P_v(t) = k_1 \left|\frac{dB}{dt}\right|^\alpha |B(t)|^{\beta - \alpha} \tag{5}$$

Then time-average loss for an arbitrary flux waveform is calculated by the following expression (the GSE):

$$\overline{P_v} = \frac{1}{T} \int_0^T k_1 \left|\frac{dB}{dt}\right|^\alpha |B(t)|^{\beta - \alpha} dt \tag{6}$$

where

$$k_1 = \frac{k}{(2\pi)^{\alpha - 1} \int_0^{2\pi} |\cos\theta|^\alpha |\sin\theta|^{\beta - \alpha} d\theta}. \tag{7}$$

Comparison of the results of (6) with experimental results [6] suggests that the potential problem noted above—the dependence of the instantaneous loss in (5) on only the instantaneous parameters—is in fact a problem in practice. Another possible choice that would be equally consistent with the Steinmetz equation for sinusoidal waveforms, but that would not depend only on instantaneous parameters, would be

$$P_v(t) = k_i \left|\frac{dB}{dt}\right|^\alpha (\Delta B)^{\beta - \alpha} \tag{8}$$

where ΔB is the peak-to-peak flux density. The expression for time-average loss then becomes

$$\overline{P_v} = \frac{1}{T} \int_0^T k_i \left|\frac{dB}{dt}\right|^\alpha (\Delta B)^{\beta - \alpha} dt \tag{9}$$
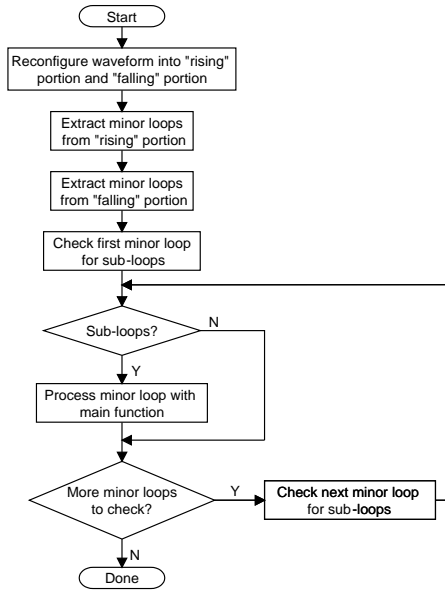
Fig. 1. Flow chart for separation of minor loops. Detail of the step in which minor loops are separated from the rising portion of the loop is shown in Fig. 2.
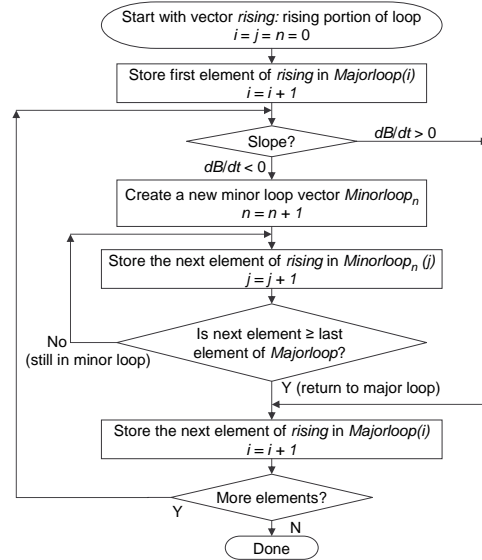

Fig. 2. Flow chart for a function used in separation of minor loops. This function removes the minor loops from the rising portion of the waveform.

where

$$k_i = \frac{k}{(2\pi)^{\alpha-1} \int_0^{2\pi} |\cos\theta|^\alpha 2^{\beta-\alpha} d\theta}. \qquad (10)$$

If, at each point in the waveform, ΔB is taken as the peak-to-peak amplitude of the major or minor loop that contains that point, this formulation can then calculate loss appropriately in the presence of minor loops.

B. Algorithm for Separation of Minor Loops

In order to apply (9) separately to each major or minor loop of a waveform in an automated CAD system, it is necessary to have an algorithm capable of splitting an arbitrary waveform in a major loop and one or more minor loops. The algorithm should be able to handle sub-loops within minor loops, sub-sub-loops within those sub-loops, and so on, for any number of nested levels.

We have developed such an algorithm and implemented it as a MATLAB function. A single cycle of a periodic piece-wise-linear (PWL) flux-density waveform is given as the input. This could correspond to a true PWL flux-density waveform, as is common in power-converter magnetics, or it could be a discretized approximation to a different type of waveform such as a sinusoid.

The sequence of steps followed in the algorithm is diagrammed in Figs. 1 and 2. First, the waveform is partitioned into two sections. The "rising" section is the portion between the lowest point in the waveform and the highest point. It may include both positive- and negative-slope portions, but it is, on average, rising. The "falling" section is the portion of the

waveform between the peak value and the minimum value. The periodic nature of the waveform is considered in locating these sections; typically at least one of the sections "wraps" to include a portion from of the tail of the input waveform preceding a portion from the start of the waveform. If more than one point in the waveform is equal to the maximum value or the minimum value, any one of the equal values can be chosen as the dividing point between the "rising" and "falling" portions.

The process of splitting the minor loops contained in the rising portion of the waveform is diagrammed in Fig. 2. The values of flux density from this portion are placed, one-by-one, into a vector, *MajorLoop*, until the start of a minor loop is detected via a change in the slope of the waveform from positive to negative. After a minor loop starts, the flux-density values are stored as elements of a new vector in what will become a collection of minor-loop vectors. Values are stored in the first minor-loop vector until the flux-density value rises back to the same value where it started decreasing (the point where the minor loop closes). Now *MajorLoop* stores a portion of the major loop and we have one additional vector $Minorloop_1$ storing the first minor loop. More values are stored again in *MajorLoop*. If a new minor loop is encountered, values for that minor loop are stored in another minor-loop vector, and our collection of minor loops grows. The process continues until the end of the "rising" portion. Now *MajorLoop* has the entire rising portion of the major loop (which is now in fact monotonically rising) and we have all the minor loops extracted from it in separate vectors, $Minorloop_n$. These minor loops may contain sub-loops, which have to be separated also, in the recursive process described later.

For the "falling" part of the waveform, the same process

is used, except with the conditions all based on the opposite slopes. At the end of this process we have the complete major loop in *MajorLoop* and each of the minor loops (with any sub-loops still embedded) in a separate vector.

Each of the minor loops is then checked for sub-loops. If a sub-loop is detected, then that minor loop is processed by a recursive call of the original function. Thus, any sub-loops present in the minor loops are eliminated. The recursive approach can handle any number of levels of nested sub-sub-loops.

C. Loss Calculation

With a set of major and minor loops, the loss of each one can be calculated according to (9). The total loss is then found by a weighted average, weighting the contribution of each by the fraction of the total period it occupies. That is,

$$P_{tot} = \sum_i P_i \frac{T_i}{T} \tag{11}$$

where P_i is the loss given by (9) for major or minor loop i, T_i is the period of loop i, and T is the total period. This is equivalent to summing the energy loss that occurs during each loop ($P_i T_i$) and dividing the total energy loss over one cycle by the total period to obtain average power loss.

The calculation of (9) in general involves performing an integral. This may be done numerically by any of many standard methods; in some cases it is also possible to do this analytically.

A particularly common type of flux waveform in power electronics is piecewise linear (PWL). For PWL waveforms, the integral in (9) may be split into one piece for each linear segment

$$\begin{aligned} \overline{P_v} &= \frac{k_i(\Delta B)^{\beta-\alpha}}{T} \int_0^T \left|\frac{dB}{dt}\right|^\alpha dt \\ &= \frac{(k_i \Delta B)^{\beta-\alpha}}{T} \sum_m \int_{t_m}^{t_m+1} \left|\frac{dB}{dt}\right|^\alpha dt \end{aligned} \tag{12}$$

where B_m is the flux density at time t_m, and ΔB is, as before, the peak-to-peak flux density of the overall loop. For each linear time segment, the slope is a constant $\frac{dB}{dt} = \frac{B_{m+1}-B_m}{t_{m+1}-t_m}$, and the result of integration is simply

$$\overline{P_v} = \frac{k_i(\Delta B)^{\beta-\alpha}}{T} \sum_m \left|\frac{B_{m+1}-B_m}{t_{m+1}-t_m}\right|^\alpha (t_{m+1}-t_m) \tag{13}$$

This result may be used directly for typical PWL waveforms found in many power electronics applications. In the case of other waveforms, such as sinusoidal waveforms, a PWL approximation of the waveform may be used with (13) to conveniently approximate (6).

We conclude that a loss calculation routine, applicable to PWL flux waveforms, or to PWL approximations of other
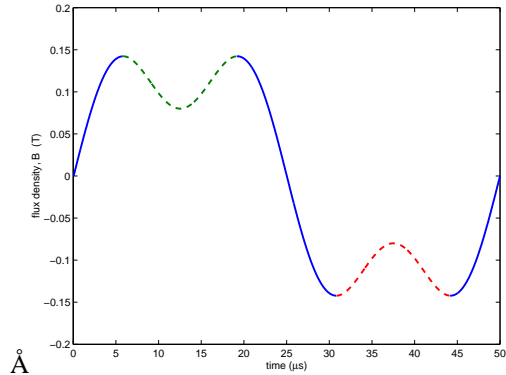

Fig. 3. An example flux waveform given by (14), with the two minor loops shown as dashed lines. This plot is for the parameter c set to $c = 0.3$.

waveforms, could be broadly useful and can be easily developed from the above analysis. First, the waveform is split into major and minor loops as described in Section II-B. Next, the loss for each major or minor loop is calculated using (13). Finally, the loss from each loop is combined using (11). We have implemented such a program in MATLAB [23] and will make it freely available [24].

III. COMPARISON WITH EXPERIMENTAL MEASUREMENTS

Core loss measurements were performed using two windings of six turns each on a toroidal core of 3C85 MnZn power ferrite (Philips), driven by a power amplifier. Current and voltage probes were used to make measurements that were processed by a digital oscilloscope to calculate power loss. Details of the measurement system are described in [6]. To examine the effect of a non-sinusoidal waveform with and without minor loops, we used a flux waveform

$$B(t) = A\left[(1-c)\sin 2\pi f t + c\sin(3 \cdot 2\pi f t)\right]. \tag{14}$$

where c is a variable parameter corresponding to the fraction of third harmonic, A is 200 mT, and $f = 20$ kHz. For $c \le 0.1$, (14) has only one major loop. But for $c > 0.1$ it has minor loops at the top and bottom of the major loop, as shown in Fig. 3.

Fig. 4 compares the results of the experiment to the MSE, to the GSE, and to our new method using (9) and accounting for minor loops—the improved GSE, labelled iGSE. We see that all fit well for $c < 0.1$ where there is only one major loop, and even up to almost $c = 0.2$ where the minor loops become significant and the GSE starts to deviate significantly. The MSE continues to match up to about $c = 0.4$ but then does not match well at all for high values of c. The iGSE, however, models the actual behavior accurately through the whole range. At high values of c, above about $c = 0.7$, the GSE and the iGSE again converge, as the waveform again approaches a single sinusoid, and the minor loops are of less importance.
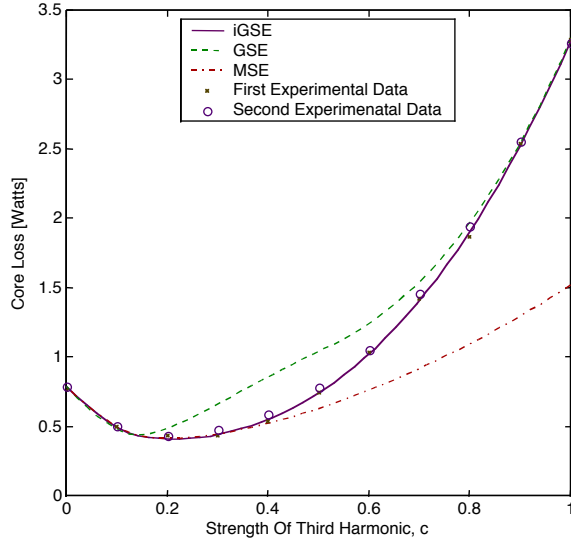
Fig. 4. Comparison of loss predicted by three models to experimental data for a flux waveform composed of two harmonically related sinusoids (14). The two sinusoids are at 20 kHz and 60 kHz, with a maximum amplitude of 200 mT.

Thus, we see that new method corrects the deviation that the GSE has from the experimental data, and is more consistently accurate than any of the previous methods.

IV. SIMPLIFIED APPLICATION

Although our primary objective was to create a model that could be used in a high-performance CAD program, we also recognize that many engineers will wish to calculate core loss by hand, or in their own programs, which in some cases will not be easily linked to our programs. For example, some may wish to use a simple spreadsheet program. For the case of PWL waveforms with no minor loops the loss may be calculated by a simple formula, requiring no integration (13). This can also be expressed in terms of the winding voltages V_j, assumed constant during each time period j of length Δt_j, as

$$\overline{P_v} = \frac{k_i (\Delta B)^{\beta - \alpha}}{T} \sum_j \left| \frac{V_j}{NA_c} \right|^\alpha (\Delta t_j), \qquad (15)$$

where N is the number of turns and A_c is the cross sectional core area. Note that ΔB is the peak-to-peak flux of the loop under consideration, not just of one segment of a piecewise-linear waveform.

The only remaining complication in applying this for simple waveforms is the need to numerically integrate $\int_0^{2\pi} |\cos \theta|^\alpha d\theta$ to find the constant k_i. To simply this operation, we have performed the numerical integration for a range of values of α from 0.5 to 3, and performed a curve fit to the results. We find that, to within 0.15%,

$$\int_0^{2\pi} |\cos \theta|^\alpha d\theta = 4 \left(0.2761 + \frac{1.7061}{\alpha + 1.354} \right). \qquad (16)$$

Thus, k_i can be expressed in terms of the Steinmetz parameters as

$$k_i = \frac{k}{2^{\beta + 1} \pi^{\alpha - 1} \left(0.2761 + \frac{1.7061}{\alpha + 1.354} \right)}. \qquad (17)$$

We conclude that with no minor loops, and piecewise linear flux waveforms, all that is needed for a simple calculation of core loss is (17) and (15).

V. LIMITATIONS AND FUTURE WORK

The improved GSE (iGSE) with separation of minor loops overcomes problems with previous methods and matches our experimental data very well. Only the Steinmetz parameters are needed; no additional measurements or curve fitting are needed. However, this is subject to several important limitations. Further work is needed to overcome these limitations.

The best-fit Steinmetz parameters are known to vary with frequency [25], [6]. For waveforms with a harmonic content over a wide frequency range, choosing the appropriate parameters can be problematic, as discussed in greater detail for the GSE in [6]. Although more complex alternatives to the Steinmetz equation have been proposed to account for this parameter variation [25], it is not clear how this can be done in the iGSE.

Ferrite core loss is known to vary with dc bias [7], [8], [9], whereas the iGSE predicts loss that is completely independent of dc bias. The GSE loss predictions do depend on dc bias, but only by accident, not by design, and dc sensitivity of the GSE appears to be significantly greater than that of actual materials. Further experimental work is needed before an accurate model of dc bias effects can be developed.

Because there are an infinite number of possible nonsinusoidal waveforms, testing the iGSE for all of them is not possible. The iGSE was developed from the Steinmetz parameters–a curve fit just to sinusoidal waveforms–and then generalized to nonsinusoidal waveforms, for which it was shown to work well. Because it was developed in this way, we have confidence that it will work reasonably well for any nonsinusoidal waveform, within the limitations of frequency range and dc bias discussed above. If instead, we had merely provided a curve fit to measured nonsinusoidal data, there would be little reason to expect that the curve fit would work well for any type of waveform that we had not measured. But the iGSE has demonstrated its ability to work for waveforms other than the sinusoids from which the parameters were generated, so it is not unreasonable to expect it to work for other nonsinusoidal waveforms. However, it is impossible to conclusively prove that the iGSE will work for any waveform without an infinite amount of data. Even though it can never be conclusively proven to be universally applicable, we would have more confidence in it with more experimental data.

As the theory of loss mechanisms in ferrite advances, it may eventually become possible to do practical loss estimation using a model with a more direct physical basis. One promising

approach that should be studied for its implications on loss with nonsinusoidal core loss is the fractal models discussed in [26], [27].

This work presently predicts only the area of the hysteresis loop, not its shape. For dynamic circuit simulation, a dynamic hysteresis model capable of simulating the full nonlinear dynamic behavior of the material is needed. We have not yet investigated developing dynamic models consistent with the iGSE loss model.

VI. CONCLUSION

We calculate core loss by separation of a flux trajectory into major and minor loops and the application of a loss calculation similar to that in [6], but with loss depending on peak-to-peak flux density instead of instantaneous flux density. The result matches experimental data well. It is the only method we know of that can accurately calculate loss with any waveform, without requiring extra characterization of material properties beyond the parameters for the Steinmetz equation.

REFERENCES

[1] S. Mulder, "Power ferrite loss formulas for transformer design", *Power Conversion & Intelligent Motion*, vol. 21, no. 7, pp. 22–31, July 1995.
[2] E. C. Snelling, *Soft Ferrites, Properties and Applications*, Butterworths, second edition, 1988.
[3] C. P. Steinmetz, "On the law of hysteresis", *AIEE Transactions*, vol. 9, pp. 3–64, 1892, Reprinted under the title "A Steinmemtz contribution to the ac power revolution", introduction by J. E. Brittain, in *Proceedings of the IEEE* 72(2) 1984, pp. 196-221.
[4] M. Albach, T. Durbaum, and A. Brockmeyer, "Calculating core losses in transformers for arbitrary magnetizing currents a comparison of different approaches.", in *PESC 96 Record. 27th Annual IEEE Power Electronics Specialists Conference*, June 1996, vol. 2, pp. 1463–8.
[5] J. Reinert, A. Brockmeyer, and R.W. De Doncker, "Calculation of losses in ferro- and ferrimagnetic materials based on the modified Steinmetz equation", in *Proceedings of 34th Annual Meeting of the IEEE Industry Applications Society*, 1999, pp. 2087–92 vol.3.
[6] Jieli Li, T. Abdallah, and C. R. Sullivan, "Improved calculation of core loss with nonsinusoidal waveforms", in *Conference Record of the 2001 IEEE Industry Applications Conference. 36th IAS Annual Meeting*, 2001, pp. 2203–2210.
[7] A. Brockmeyer, "Experimental evaluation of the influence of dc-premagnetization on the properties of power electronic ferrites", in *APEC '96. Eleventh Annual Applied Power Electronics Conference*, 1996, pp. 454–60.
[8] A. Brockmeyer and J. Paulus-Neues, "Frequency dependence of the ferrite-loss increase caused by premagnetization", in *Twelfth Annual Applied Power Electronics Conference and Exposition*, 1997, pp. 375–80.
[9] Wai Keung Mo, D.K.W. Cheng, and Y.S. Lee, "Simple approximations of the dc flux influence on the core loss power electronic ferrites and their use in design of magnetic components", *IEEE Transactions on Industrial Electronics*, vol. 44, no. 6, pp. 788–99, 1997.
[10] G. Bertotti, "General properties of power losses in soft ferromagnetic materials", *IEEE Transactions on Magnetics*, vol. 24, no. 1, pp. 621–630, 1988.
[11] G. Bertotti, *Hysteresis in magnetism: for physicists, materials scientists, and engineers*, Academic Press, 1998.
[12] K. H. Carpenter, "Simple models for dynamic hysteresis which add frequency-dependent losses to static models", *IEEE Transactions on Magnetics*, vol. 34, no. 3, pp. 619–22, 1998.
[13] J.-T. Hsu and K.D.T Ngo, "A Hammerstein-based dynamic model for hysteresis phenomenon", *IEEE Transactions on Power Electronics*, vol. 12, no. 3, pp. 406–413, 1997.
[14] H. Saotome and Y. Sakaki, "Iron loss analysis of mn-zn ferrite cores", *IEEE Transactions on Magnetics*, vol. 33, no. 1, pp. 728–34, 1997.
[15] W. Roshen, "Ferrite core loss for power magnetic components design", *IEEE Transactions on Magnetics*, vol. 27, no. 6, pp. 4407–15, 1991.
[16] P. Tenant and J. J. Rousseau, "Dynamic model of magnetic materials applied on soft ferrites", *IEEE Transactions on Power Electronics*, vol. 13, no. 2, pp. 372–9, 1998.
[17] F. Fiorillo and A. Novikov, "An improved approach to power losses in magnetic laminations under nonsinusoidal induction waveform", *IEEE Transactions on Magnetics*, vol. 26, no. 5, pp. 2904–10, 1990.
[18] D.C. Jiles, "Frequency dependence of hysteresis curves in 'non-conducting' magnetic materials", *IEEE Transactions on Magnetics*, vol. 29, no. 6, pp. 3490–2, 1993.
[19] A. Brockmeyer, *Dimensionierungswekzeug für magnetische Bauelemente in Stromrichteranwendungen*, PhD thesis, Aachen University of Technology, 1997.
[20] Jinjun Liu, T.G. Wilson, Jr., R.C. Wong, R. Wunderlich, and F.C. Lee, "A method for inductor core loss estimation in power factor correction applications", in *Proceedings of APEC 2002 - Applied Power Electronics Conference and Exposition*, 2002, p. 439.
[21] M.S. Lancarotte and A. de Arruda Penteado, Jr., "Estimation of core losses under sinusoidal or nonsinusoidal induction by analysis of magnetization rate", in *Electric Machines and Drives International Conference IEMD '99*, 1999, pp. 490–492.
[22] I.D. Mayergoyz, *Mathematical models of hysteresis*, Springer-Verlag, 1991.
[23] The MathWorks, Inc., http://www.mathworks.com, *MATLAB Version 6*, 2000.
[24] *Dartmouth Magnetic Component Research Web Site*, http://engineering.dartmouth.edu/inductor.
[25] R. Ridley, "Modeling ferrite core losses", *Switching Power Magazine*, vol. 3, no. 1, pp. 6–13, 2002.
[26] V. Vorperian, "A fractal model of anomalous losses in ferromagnetic materials", in *23rd Annual IEEE Power Electronics Specialists Conference*, 1992, vol. 2, pp. 1277 –1283.
[27] V. Vorperian, "Using fractals to model eddy-current losses in ferromagnetic materials", *Switching Power Magazine*, vol. 3, no. 1, pp. 18–27, 2002.